



Originally published as:

Heine, C., Müller, D., Steinberger, B., DiCaprio, L. (2010): Integrating deep Earth dynamics in paleogeographic reconstructions of Australia. - *Tectonophysics*, 483, 1-2, 135-150

DOI: [10.1016/j.tecto.2009.08.028](https://doi.org/10.1016/j.tecto.2009.08.028).

Integrating deep Earth dynamics in paleogeographic reconstructions of Australia

Christian Heine ^{a,1}, R. Dietmar Müller ^a, Bernhard Steinberger ^b,
Lydia DiCaprio ^a,

^a*EarthByte Group, School of Geosciences, The University of Sydney, NSW 2006,
Australia*

^b*Center for Geodynamics, Norges Geologiske Undersøkelse (NGU), Trondheim,
Norway*

Abstract

It is well documented that the Cenozoic progressive flooding of Australia, contemporaneous with a eustatic sea level fall, requires a downward tilting of the Australian Plate towards the SE Asian subduction system. Previously, this large-scale, mantle-convection driven dynamic topography effect has been approximated by computing the time-dependent vertical shifts and tilts of a plane, but the observed subsidence and uplift anomalies indicate a more complex interplay between time-dependent mantle convection and plate motion. We combine plate kinematics with a global mantle backward-advection model based on shear-wave mantle tomography, paleogeographic data, eustatic sea level estimates and basin stratigraphy to reconstruct the Australian flooding history for the last 70 Myrs on a continental scale. We compute time-dependent dynamic surface topography and continental inundation of a digital elevation model adjusted for sediment accumulation. Our model reveals two evolving dynamic topography lows, over which the Australian plate has progressively

moved. We interpret the southern low to be caused by sinking slab material with an origin along the eastern Gondwana subduction zone in the Cretaceous, whereas the northern low, which first straddles northern Australia in the Oligocene, is mainly attributable to material subducted north and northeast of Australia. Our model accounts for the Paleogene exposure of the Gulf of Carpentaria region at a time when sea level was much higher than today, and explains anomalous Late Tertiary subsidence on Australia's northern, western and southern margins. The resolution of our model, which excludes short-wavelength mantle density anomalies and is restricted to depths larger than 200 km, is not sufficient to model the two well recorded episodes of major transgressions in South Australia in the Eocene and Miocene. However, the overall, long-wavelength spatio-temporal pattern of Australia's inundation record is well captured by combining our modelled dynamic topography with a recent eustatic sea level curve. We suggest that the apparent Late Cenozoic northward tilting of Australia was a stepwise function of South Australia first moving away northwards from the Gondwana subduction-related dynamic topography low in the Oligocene, now found under the Australian-Antarctic Discordance, followed by a drawing down of northern Australia as it overrode a slab burial ground now underlying much of the northern half of Australia, starting in the Miocene. Our model suggests that today's geography of Australia is strongly dependent on mantle forces. Without mantle convection, which draws Australia down by up to 300m, nearly all of Australia's continental shelves would be exposed. We conclude that dissecting the interplay between eustasy and mantle-driven dynamic topography is critical for understanding hinterland uplift, basin subsidence, the formation and destruction of shallow epeiric seas and their facies distribution.

Key words: Australia, dynamic topography, Paleo-DEMs, inundation patterns, plate motions, Cenozoic

¹ corresponding author; now at StatoilHydro, Global Exploration Technology,

1 Introduction

1

The motions of continents relative to large scale patterns of mantle convection can contribute to the creation and destruction of sediment accommodation space due to transient, dynamic displacement of the surface topography, usually referred to as dynamic topography (Lithgow-Bertelloni and Gurnis, 1997; Gurnis et al., 1998; Burgess and Gurnis, 1995; Gurnis, 1990). A significant dynamic topography effect has been demonstrated in particular for Cretaceous and Cenozoic Australian continental paleogeography based on the misfit between the global flooding patterns and the Australian continental flooding, which appears to be out-of-sync with eustasy (DiCaprio et al., 2009; Sandiford, 2007; Veevers, 2001; Gurnis et al., 1998; Russell and Gurnis, 1994). Large-scale, mantle-driven dynamic topography can be approximated by the time-dependent vertical shifts and tilts of a plane, computed from the displacement needed to reconcile the interpreted pattern of marine incursion with a predicted topography in the presence of global sea level variations (DiCaprio et al., 2009). However, some observed subsidence and uplift anomalies, particularly along the south coast of Australia (DiCaprio et al., 2009; Sandiford, 2007), indicate a more complex interplay between time-dependent mantle convection and plate motion than that approximated by vertical shifts and tilts of a plane.

2
3
4
5
6
7
8
9
10
11
12
13
14
15
16
17
18
19
20

Geodynamic models predict between a few hundred meters and up to 2 km of surface vertical motion in response to mantle dynamic processes (Müller et al., 2008b; Conrad et al., 2004; Conrad and Gurnis, 2003; Lithgow-Bertelloni and Silver, 1998; Lithgow-Bertelloni and Gurnis, 1997; Gurnis et al., 1998; Russell

21
22
23
24

Drammensveien 264, N-0246 Oslo, Norway; Email: c.heine@usyd.edu.au

and Gurnis, 1994; Mitrovica et al., 1989). Depending on the tomography model
used to infer mantle density heterogeneities, Steinberger (2007) found 0.4–1.0
km rms amplitude, when converting vertical stresses to elevation beneath air,
compared to 0.4–0.5 km for residual topography (i.e., observed topography
corrected for crustal thickness variations and variations in ocean floor age).
However, the surface expression of subducted slabs in Southeast Asia is half
an order of magnitude smaller than predicted by dynamic topography models
(e.g. Wheeler and White, 2000), having an upper bound of only ≈ 300 m. This
has been interpreted as indication that mantle mass anomalies are supported
elsewhere, presumably at internal boundaries within Earth.

Here we use a simple mantle backward advection model to unravel the contri-
bution of mantle convection-induced dynamic topography to the paleogeogra-
phy of the Australian continent over the last 70 Ma. Published Australian paleo-
geographic and geological data are used to match modelled paleo-topography,
focusing on the evolution of the large-scale spatial distribution of anomalous
subsidence and uplift and to provide better constraints on the amplitudes of
mantle-induced topography. Our method facilitates the quick evaluation of
global and regional dynamic topography models with geological observations.

2 Australian Cenozoic Paleogeography: key regions for this study

The Australian continent is characterised by large areas of low elevation
(Fig. 1), making it an excellent natural laboratory for investigating the effects
of eustasy and mantle convection on paleogeography. Rifting along Australia’s
southern margin and the Tasman Sea opening commenced in the Early Cre-
taceous and early Late Cretaceous, respectively (Norvick and Smith, 2001;

[Gaina et al., 1998](#)). The main, syn-rift subsidence started along the western 1
parts of the southern margin in the Late Jurassic and propagated eastward 2
with thermal, post-rift subsidence commencing around 110–80 Ma ([Norvick 3
and Smith, 2001](#); [Brown et al., 2001](#)). The thermal effects of rifting had likely 4
dissipated by the beginning of the Tertiary along the central southern margin, 5
hence can be largely disregarded for this study. 6

The Australian plate has undergone major changes in plate boundary forces 7
throughout the Tertiary, which profoundly affected the evolution of the in- 8
traplate stress field through time, causing reactivation along pre-existing struc- 9
tures or weaknesses ([Dyksterhuis and Müller, 2008](#); [Dyksterhuis et al., 2005](#); 10
[Sandiford et al., 1995](#)). Examples where this might have had an effect on 11
the local topography due to significant deformation are the tectonically ac- 12
tive Flinders / Mt. Lofty Ranges ([Dyksterhuis and Müller, 2008](#); [Célerier 13
et al., 2005](#); [Sandiford, 2003b](#), Fig. 1) and the Otway Ranges ([Dyksterhuis 14
and Müller, 2008](#); [Sandiford, 2003a,b](#)). Collisional processes along the eastern 15
and northern margins of the Australian plate are reported to start around 16
Oligocene time in New Caledonia, Papua New Guinea ([Cluzel et al., 2001](#); 17
[Schellart et al., 2006](#)) and, later, in the New Zealand region between 25–20 18
Ma ([Schellart, 2007](#); [Kamp, 1986](#), and references therein) and along the north- 19
ern Australian margin ([Hinschberger et al., 2005](#); [Hall and Wilson, 2000](#); [Hall, 20
1998](#)). The effects from foreland loading due to orogeny prove to be negligible 21
because of the distance from the flexural load as modelling by [Müller et al. 22
\(2000b\)](#) has demonstrated. Subsidence due to changes in the far field and in- 23
traplate stress field are considered to produce elongated, asymmetric patterns 24
([Nielsen et al., 2007, 2005](#)) and are not evident from available Australian data. 25
Here, we focus on subsidence and uplift anomalies at large wavelengths (1000 26

kilometers and more) which cannot have their origin in structural reactivation
or flexure.

The various departures of the Cenozoic Australian flooding history from global
eustatic curves have been pointed out by [Veevers \(1984\)](#) and contributors who
realised a significant misfit between continental inundation patterns and the
eustatic sea level estimate of [Bond \(1978\)](#). Figure 2 shows the eustatic sea level
estimate of [Haq and Al-Qahtani \(2005\)](#) plotted versus the inundation of the
Australian continent for the last 70 Ma. The inundation is determined by the
flooded continental area relative to the present-day 200 m isobath. Whereas
the eustatic sea level estimates all show a gradual decrease, the inundation
of Australia increases from around 5% in early Paleocene to about 25% at
present (Fig. 2).

Focusing on the Murray and Eucla Basins along the south coast of Australia
(Fig. 1) we investigate anomalies in Cenozoic inundation patterns and their
origin utilising a recent eustatic sea level curve [Haq and Al-Qahtani \(2005\)](#).
In middle Miocene times (< 11 Ma), [Veevers \(1984\)](#) describes the following
anomalies based on a sea level which corresponds to the present-day 20 m
contour (80 m according to [Haq and Al-Qahtani, 2005](#)), assuming a constant
hypsometry.

- In the Nullarbor Plain (Fig. 1), shallow marine middle Miocene limestone
slopes occur from an elevation of +200 m inland towards 0 m at the coast,
indicating uplift since deposition of about 180 m by tilting about a hinge
near the coast. If 80 m is used as reference sea level, the inland limestone
section would have been uplifted about 120 m with the coastal parts being
about 50-60 m too low.

- In the Murray Basin (Fig. 1) the top of mid-Miocene shallow marine limestone and clay has an elevation of 0 m in the east and -80 m in the west, indicating subsequent subsidence of at least 100 m about a hinge on the eastern side of the basin. Using the [Haq and Al-Qahtani \(2005\)](#) estimate, the deposits in the western part must have subsided about 160 m.
- The Lake Eyre region (Fig. 1), today at 12 m below sea level, was not covered by the Miocene sea which rose +20 m (or +80 m according to [Haq and Al-Qahtani \(2005\)](#)) above the present sea level. The top of the Miocene lacustrine–fluvial Etadunna Formation is today found at -17 m implying subsidence of about 40 m or 100 m using [Haq and Al-Qahtani \(2005\)](#).
- In the Cape Range area (Fig. 1) of Western Australia’s onshore Carnarvon Basin, Mid-Miocene shallow marine limestone are now found at elevations of +300 m, implying local uplift of 280 m (220 m, [Haq and Al-Qahtani \(2005\)](#)) since deposition.

For the Eocene–Miocene times (38-24 Ma), [Veevers \(1984\)](#) assumes a sea level of 75 m above present ([Bond, 1978](#)), whereas the work of [Haq and Al-Qahtani \(2005\)](#) indicates a sea level of 220–180 m for this time:

- In south-western Australia, Late Eocene shallow marine sediments now have an elevation of +250 m near Norseman, resulting in a net uplift of 175 m (30–70 m according to [Haq and Al-Qahtani, 2005](#)). At the northern edge of Eucla Basin, along the western and north-eastern margins and off north-eastern Queensland, the Eocene and Miocene shorelines coincide, indicating a subsidence of 55 m (Haq curve: 100-140 m) in the Oligocene.
- In the Lake Eyre area, the top of the Eocene non-marine Eyre Formation has an elevation of -60 m, implying subsidence of at least 135 m (240–280 m) since the Eocene, comprising at least 60 m in the Oligocene ($\approx 5\text{m/Ma}$)

according to [Veevers, 1984](#)). 1

- In the Renmark area of the Murray Basin, the top of the Late Eocene shallow 2
marine clay has an elevation of -200 m, indicating 275m (\approx 380–420 m) of 3
subsidence since the Eocene. 4

In summary, there are numerous localities along the Australian continental 5
margins and in the interior where eustatic sea level variations and local tec- 6
tonics alone can not explain the large scale inundation and vertical motion 7
patterns recorded in Australia’s Cenozoic geologic record. This indicates that 8
other, large-scale dynamic processes must have taken place to account for 9
the observed deviations. As Australia separated from Antarctica, it started 10
to move away from residual Gondwana slab material in the upper mantle 11
in the area that later became the Australian-Antarctic Discordance ([West 12
et al., 1997](#); [Gurnis et al., 1998](#)), and towards the south-east Asian slab burial 13
grounds ([Gaina and Müller, 2007](#); [Müller et al., 2000a](#)). This in turn resulted 14
in a time-dependent surface topography that dynamically adjusted itself rel- 15
ative to its changing position with respect to mantle up- and downwellings 16
([Gurnis, 2001](#)). [Veevers \(2001\)](#) suggested that this process was a principal 17
cause for the anomalous subsidence and uplift patterns which are reported for 18
various times in the younger geological record of Australia [Veevers \(2001\)](#). 19

3 Methodology 20

3.1 Mantle Convection and Dynamic topography model 21

Seismic tomography captures information about the present day distribution 22
of materials that produce fast and slow perturbations to a reference earth 23

velocity model. Velocity variations relate to both thermal and compositional 1
variations, both of which affect buoyancy. Commonly it is assumed that rel- 2
atively higher seismic velocities indicate colder material downwelling whereas 3
areas of lower seismic velocities indicate hotter material upwelling (e.g. [Grand 4](#)
[et al., 1997](#); [van der Hilst et al., 1997](#)). 5

Using a well established global mantle convection modelling approach, we com- 6
pute the time-dependant surface topography for the last 70 Myrs by advecting 7
density anomalies back in the mantle flow field ([Steinberger, 2007](#); [Xie et al., 8](#)
[2006](#); [Steinberger et al., 2004](#)). We use a global, self-consistent plate kine- 9
matic model ([Müller et al., 2008a](#)), based on a moving hotspot absolute plate 10
motion reference frame ([O’Neill et al., 2003](#)), to impose surface plate motion 11
constraints on the mantle convection model. Relative density anomalies are 12
derived by converting relative seismic velocities from the global global S20RTS 13
seismic tomographic model ([Ritsema et al., 1999](#)) using an empirical conver- 14
sion factor of 0.25 below depths of 220 km. This velocity-to-density scaling 15
factor is based on a good fit with the observed geoid and consistent with 16
mineral physics ([Karato, 1993](#); [Steinberger and Calderwood, 2006](#)). We as- 17
sume that both seismic velocity and density anomalies in the sub-lithospheric 18
mantle are due to temperature changes, and hence perfectly correlated. 19

According to the isopycnic hypothesis, seismic velocity variations in the con- 20
tinental lithosphere do not correspond to density variations, or correspond to 21
only very small density variations [Jordan \(1978, 1988\)](#); [Shapiro et al. \(1999\)](#). 22
Excluding a heterogeneous lithosphere (upper 220 km) thus avoids gross over- 23
estimation of dynamic topography amplitudes ([Steinberger et al., 2001](#)). How- 24
ever, parts of the Australian lithosphere indicate that deep lithospheric keels 25
and potential compositional heterogeneities might extend deeper than 220 km 26

(Fishwick et al., 2008; Artemieva, 2003) and be responsible for over-prediction
of the dynamic topography amplitude. Conversely, in regions near the coast,
where the lithosphere is thin, calculations would probably be more accurate
if some velocity perturbations shallower than 220 km were used as well.

The flow field of the mantle for the last 70 Ma is calculated using a spectral
method (Hager and O’Connell, 1981), by spherical harmonic expansion of
surface plate velocities and internal density heterogeneities at each depth level
(Steinberger et al., 2004; Xie et al., 2006; Steinberger and Calderwood, 2006).
The viscosity model (Steinberger et al., 2004) considers only radial viscosity
variations and is based on mineral physics and obtains a good fit globally
with the geoid and other observations. The model is constrained by matching
paleo-latitudes of hotspots from paleomagnetic data and geometry and age
progression along hotspot tracks. The change of mantle density anomalies with
time is computed by advecting them back in the mantle flow field through time
as a function of their buoyancy (Steinberger et al., 2004).

From the backward-advected density models, the vertical stress at the upper
boundary is computed. Here a horizontal stress-free boundary condition is
used on the upper boundary of the high-viscosity lithosphere (2.4×10^{22} Pa s).
Vertical stresses are converted to topography with a density contrast of 3.3
g/cm³. That means, the dynamic topography computed here is appropriate
for “beneath air”.

The model output is relative to the geoid (i.e. relative to sea level). We limit
our backward-advected models to the past 70 Myrs, which is about the time
span for which present-day mid-mantle structure can be reconstructed reason-
ably well using a backward-advection analytical flow model.

Long-term fluctuations of the global sea level through geological time are primarily caused by changes in the volume of the ocean basins and fluctuating inland ice volume. These have long been recognised through their effect on depositional patterns on continental platforms and margins (Bond, 1978; Hallam, 1984; Watts and Thorne, 1984; Haq et al., 1987; Sahagian and Watts, 1991; Sahagian and Jones, 1993; Miller et al., 2005). Eustasy provides an important constraint for modelling epeirogenic and tectonic motion from flooding patterns. Over the past 30 years several attempts have been made to generate eustatic sea level curves (Müller et al., 2008b; Haq and Al-Qahtani, 2005; Haq et al., 1987; Miller et al., 2005; Sahagian et al., 1996) with little consensus reached up to the mid 1990's (Miall, 1992; Christie-Blick and Driscoll, 1995).

Recent work estimating the eustatic sea level through computing the volume of ocean basins through time in combination with dynamic topography models (Müller et al., 2008b) suggests that eustatic sea level estimates based on the New Jersey margin (e.g. Miller et al., 2005; Watts and Thorne, 1984) are significantly underestimated, due to the effect of mantle-driven dynamic topography on the east coast of North America during the Tertiary (Spasojević et al., 2008; Müller et al., 2008b). Müller et al. (2008b) demonstrated that the eustatic sea level amplitudes and long-time trend based on ocean basin volume changes are similar to the Haq and Al-Qahtani (2005) curve (Fig. 2). We have hence chosen the latter curve as eustatic sea level input for our models. The Haq and Al-Qahtani (2005) curve represents an updated version of the original Meso- and Cenozoic eustatic sea level chronology (Haq et al., 1987), recalibrated to the numerical Geologic Time Scale 2004 (Gradstein et al., 2004).

Digital paleogeographic maps from *The Paleogeographic Atlas of Australia – Vol. 10 Cainozoic* (Langford et al., 1995) were used to empirically scale the dynamic topography input to optimise the agreement between modelled and observed paleo-topography, as explained in section 3.4. The compilation of Langford et al. (1995) contains geological data for the Cenozoic which is averaged for individual time slices with varying duration of 3-19.6 Ma (Supplementary material, Table 1). Struckmeyer and Brown (1990) interpreted the depositional environment of a total of 361 data points, providing the base for Langford et al.’s work who grouped the data into digital sets of georeferenced polygons, according to broad paleo-environment characteristics (e.g “land erosional” or “marine shallow”). We have combined all polygons classified as “land” to reconstruct a coherent continent-wide paleo-shoreline for each time slice to derive the amount of flooding. We excluded time slices 7 (Pleistocene) and 8 (Holocene) due to the spatio-temporal resolution of our model. It is important to remark that the data from Langford et al. (1995) represents the maximum extent of a distinct paleogeographic environment integrated over each given time interval. Ages from the paleogeographic atlas are based using the Berggren et al. (1995) time scale. These were converted to the GTS2004 time scale (Gradstein et al., 2004). We accounted for sediment deposition by backstripping the sediments at available datapoints Langford et al. (1995, c.f.) and isostatically correcting the topographic base level of our model. The backstripping technique as outlined by Steckler and Watts (1978), is used to isolate the effects of sediment loading from the tectonic subsidence of the basement by restoring and subsequently removing the decompacted

sediment thickness at time of deposition (Allen and Allen, 2005; Sclater and
Christie, 1980):

$$Y = S \frac{\rho_m - \bar{\rho}_s}{\rho_m - \rho_w} \quad (1)$$

where Y is the isostatic correction, ρ_m and ρ_w the densities of mantle rocks and
water, respectively, and S the thickness of the decompacted sedimentary unit,
 $\bar{\rho}_s$ is the average density for the sedimentary unit. Local 1D backstripping was
applied to each datapoint to account for sediment deposition and to restore
the appropriate surface elevation using Airy isostasy.

Due to relatively thin Cenozoic sediment thicknesses, large regional extend of
the deposits, and high elastic thickness values of the Australian lithosphere
(Swain and Kirby, 2006; Simons and van der Hilst, 2002), flexural effects
from sedimentary loading are negligible and Airy-type compensation can be
assumed. The individual data points with decompacted sections were gridded
for the individual time slices using a continuous curvature fitting gridding
algorithm (Wessel and Smith, 1998). It is assumed that elevations above the
present-day 300 m contour have been dominantly erosional with insignificant
amounts of sediment being deposited.

In areas without hydrocarbon prospectivity, most of the Cenozoic datapoints
lack accurate stratigraphic thickness information for individual time steps.
The absence of coherent sequence stratigraphic frameworks for the onshore
Cenozoic in Australia, for example the Eucla Basin (cf. Clarke et al., 2003)
might have complicated the regional data compilation and could be one cause
for erroneous stratigraphic interval information. We have checked the values
reported by Langford et al. (1995) against the Geoscience Australia National

Petroleum wells database (<http://dbforms.ga.gov.au/www/npm.well.search>,
1
accessed 2009-02-10) and published stratigraphic data for the locations used
2
for backstripping and topographic modelling (Figs. 6 and 5).
3

3.4 Methodology, model calibration, and scaling 4

We assume that the present-day topography of Australia (N.O.A.A., National
5
Geophysical Data Center, 2006, Fig. 3a) contains mantle-driven topography
6
components, which are represented by our dynamic topography model for the
7
present (Fig. 3b). To obtain a topography without mantle-driven components
8
as base grid (Fig. 3c), we subtract the present-day dynamic topography signal
9
from the digital elevation model (DEM) of Australia. Subsequently, dynamic
10
topography models for the last 70 Myrs are rotated into the fixed present-
11
day Australian position using the EarthByte rotation model (Müller et al.,
12
2008a) and merged with the “non-dynamic” base DEM grid. The procedure
13
is repeated in 1 m.y. intervals, effectively evaluating the difference between
14
dynamic topography estimates between the time steps. Sediment-unloading
15
corrections are applied to the surface elevation estimates for the Australian
16
region to account for sediment deposition through time. The eustatic sea level
17
estimate for any given time is then added to the grid to obtain a paleo-DEM.
18

The paleo-shoreline positions derived from the environment-polygons of Lang-
19
ford et al. (1995) are then used to achieve a best fit match of the reconstructed
20
paleogeography by empirically scaling the dynamic topography model output
21
grids using an iterative approach. A series of reconstructions for a range of scal-
22
ing factors was made and their fit analysed over the 70 timesteps. Most weight
23
has been assigned to the fit with paleogeographic data in low-lying regions
24

which have been tectonically stable over the last 70 Myrs, having recorded 1
transgressive and regressive cycles in the sedimentation record. These were 2
the Murray Basin, the Eucla Basin, the Gulf of Carpentaria and parts of the 3
North West Shelf. Most emphasis was put on a regional evaluation of a best 4
fit, i.e. matching general patterns of regression and transgression, and flood- 5
ing and uplift over the entire Australian region rather than attempting to fit 6
individual key sections. However, it is important to note that in areas of low 7
topographic gradients, our predicted shoreline position is highly susceptible 8
to errors as little changes in elevation here will result in large changes in the 9
coastline location. 10

An empirical scaling factor of 0.55 for the dynamic topography model was 11
found to yield the best match between the paleogeographic data and mod- 12
elled flooding patterns on continent-scale. The necessity for downscaling the 13
raw dynamic topography field probably primarily reflects shortcomings of the 14
currently used conversion of mantle seismic shear-wave velocities to density 15
anomalies: 16

(1) Not all seismic velocities variations below 220 km are of thermal origin. 17

In the current analytical approach all seismic shear wave velocity anoma- 18
lies are converted to density anomalies with the same conversion factor 19
corresponding to thermal anomalies. However, the existence of chemical 20
heterogeneities, especially in the lower mantle, has clearly been demon- 21
strated (Trampert et al., 2004). Therefore, using a thermal scaling factor 22
may not always be appropriate. In areas with a thick tectosphere, seismic 23
velocity anomalies in the upper mantle might also be related to chemical 24
boundary layers and compositional heterogeneities extending deeper than 25
220 km (Shapiro et al., 1999). This is probably the case for some parts 26

of the Australian lithosphere (Fishwick et al., 2005, 2008; Stoddard and Abbot, 1996).

- (2) Further, the procedure of backward-advecting converted seismic velocity anomalies through time yields potential problems as it does not account for heat diffusion. A shallow negative seismic anomaly, for example, is computed to occur at greater depths back through time, causing *less* dynamic topography in the past. In reality, this would have occurred only if the associated upwelling had only recently arrived beneath the lithosphere. If the upwelling had been there for longer time it might have been stronger in the past, which would, to the contrary of what is computed in the model, result in dynamic subsidence (Xie et al., 2006). Hence, dynamic topography and its changes through time are difficult to predict from backward-advection models and the results should be treated with the appropriate caution.

In addition, predicted dynamic topography depends on viscosity structure, which is uncertain. The structure adopted here is meant to represent a global average, yet regional variations almost certainly exist. In particular, it is not well known how pronounced a low-viscosity asthenosphere there is beneath Australia, i.e. how thick it is and what is the minimum viscosity. Also, some viscous stresses may be supported on deep interfaces (Wheeler and White, 2000). The nature of such interfaces is currently unknown, and including the main known phase boundaries with their experimentally determined parameters has been shown to be insufficient to achieve a sufficiently substantial reduction in dynamic topography (Steinberger, 2007). Hence the additional scaling factor may also be viewed as an “ad hoc” implementation of the effect of unknown deep interfaces.

4 Modelling Australia's Cenozoic paleogeography

1

By combining results from topographic reconstructions using the eustatic sea
level variations, dynamic topography and plate kinematics, the effects of man-
tle dynamics on the paleogeography can be clearly demonstrated. Throughout
the Cenozoic, dynamic topography has had considerable impact on the inun-
dation history of the Australian continent. The mantle convection-induced
surface deflection resulted in a transient, complex dynamic warping of the re-
gion. Comparing the modelling results with published paleogeographic maps,
it is possible to correlate large-scale patterns of dynamic up- and downwelling
with areas of uplift or subsidence on the Australian continent.

2
3
4
5
6
7
8
9
10

4.1 Paleocene–Early Eocene (66.4–52 Ma)

11

Paleogeographic data for the Paleocene–Early Eocene suggest that the Aus-
tralian region was mostly emergent above sea level and that the Latest Cre-
taceous/Early Paleocene coastline lay well seaward beyond the present-day
coastline (Fig. 4a; McGowran et al., 2004; Veevers, 2001; Langford et al.,
1995), although eustatic sea levels fluctuated around 220 m above the present
level (Haq and Al-Qahtani, 2005, Fig. 2).

12
13
14
15
16
17

Our dynamic topography models suggests that from the beginning of the Pa-
leocene to Early Eocene, Australia gradually moved over a dynamic topogra-
phy low situated below the northwestern half of the continent, due to slow (36
mm/yr) northwestward absolute motion of Australia from 65–45 Ma (Fig. 4a;
Whittaker et al., 2007). The low has a minimum amplitude of around -150 m
at 61 Ma. The southwestern part and eastern half of the Australian continent

18
19
20
21
22
23

are affected by positive dynamic topography, with a regional high situated 1
below southeastern Australia having an amplitude of up to 150 m (Fig. 4a). 2

The paleo-DEM for the Paleocene largely corresponds to the geological ob- 3
servations along the western, southern and eastern segments of the margin, 4
with major mismatches in northern Australia (Fig. 4a). Our modelled topog- 5
raphy for the North West Shelf margin shows slightly overestimated water 6
depths (50–100m), resulting in a more landward position of the shoreline as 7
compared to [Langford et al. \(1995\)](#). In the Great Australian Bight, predicted 8
water depths are overestimated with the model shoreline located significantly 9
landward with respect to the reported shoreline during this interval, how- 10
ever, northern parts of the Eucla Basin are modelled as exposed in accordance 11
with observations ([Hou et al., 2006, 2008](#)). The Murray Basin is modelled as 12
southward dipping, low-lying depression, suggesting a good fit with an ob- 13
served depositional fluvio-lacustrine/marginal marine environment where the 14
sand- and claystones and interbedded coals of the Renmark group cover Pre- 15
Tertiary basement ([Roy et al., 2000](#); [Langford et al., 1995](#); [Veevers, 1984](#)). The 16
Gulf of Carpentaria is modelled as subaerially exposed at elevations of around 17
200-300 m, forming a broad northward trending depression. Paleogeographic 18
data indicates a large, low-lying fluvial depositional system occupying the 19
Gulf of Carpentaria region, opening northwards into the proto-Arafura Sea. 20
Along the northern margin our model overestimates elevations compared to 21
reported paleo-shoreline positions. We relate this to the poor sediment thick- 22
ness data coverage in this frontier region, resulting in an underestimation of 23
the computed isostatic correction. 24

A circum-Pacific plate tectonic reorganisation in Early Eocene times caused a change in plate motion direction for the Australian plate from NW to NNE and dramatic increase in plate velocities to around 48 mm/yr relative to the underlying mantle (Whittaker et al., 2007; Müller et al., 2000a, Fig. 4b). The center of the modelled dynamic topography low is shifted below central Australia/Eucla Basin and amplitudes increased to around -200 m (Fig. 4b). Contemporaneously, predicted dynamic topography amplitudes in the eastern and southeastern parts of the Australian region decrease by around 50-100 m, whereas our model suggests a ≈ 200 m uplift of the North West Shelf region due to dynamic topography. Eustatic sea level lowered and fluctuated around 200 m (Fig. 2).

In the Gulf of Carpentaria observations indicate a retreat of the coastlines southwards, generating broad floodplains (Langford et al., 1995). Our modelled paleogeography for the Eocene (43 Ma; Fig. 4b) shows a near-circular depression of the central Gulf of Carpentaria region with elevations below 50 m. The modelled topography is generally over-predicted (cf. Sec. 4.1) positioning the modelled coastline significantly too far north. Along the North West Shelf observed shorelines still lie well outboard of the present-day coastline, except in the Carnarvon Basin where the present-day onshore parts are flooded, which is well predicted by our paleo-elevation model. Along the western, southwestern and eastern Australian margins, including the Queensland Plateau, geological data indicate coastline positions well outboard of the present-day coastline which is matched well by our model (Fig. 4b). In most parts of the Great Australian Bight margin we overestimate elevations with the coastline being

modelled max. 500 km too far oceanward and most of the Eucla Basin as sub-
aerially exposed. Here, sediments indicate a dramatic transgression, flooding
nearly all of the present day Eucla Basin up to its northern margin (de Broek-
ert and Sandiford, 2005; Langford et al., 1995). The modelled topography for
the Eucla Basin, however, is below 50m. Similarly to the Gulf of Carpentaria,
the accuracy of sediment thickness data in this frontier region will have sig-
nificant effects on the model outcome. In the Murray Basin, the model yields
a reasonable fit with the observations, indicating large areas below 10 m el-
evation. This is well in agreement with the observation of a minor marine
inundation deposition of shallow-marine and marginal marine/lacustrine sed-
iments (Roy et al., 2000). In the Lake Eyre region, non-marine units of the
Eyre Formation are deposited (Veevers, 2001; Langford et al., 1995).

4.3 Late Eocene – Early Oligocene (36.6–30 Ma)

During the Late Eocene – Oligocene time Australia continued to move north-
wards toward the SE Asian subduction zone system at high velocities of around
68 mm/yr (Fig 4c). Our model indicates that the leading northern edge of the
Australian plate became increasingly affected by increasing negative dynamic
topography, placing the Gulf of Carpentaria and York Peninsula over the
Melanesian slab burial ground. Amplitudes of the dynamic topography low
beneath the Eucla basin increase to around -250 m leading to the develop-
ment of an E-W striking arch of lower negative dynamic topography across
Australia (Fig 4c).

The Early Oligocene is characterised by a sea level lowstand at upper Early
Oligocene times. Shorelines retreat to the outer continental shelf all around the

continent as indicated by unconformities (Langford et al., 1995), and climatic 1
conditions change in response to the opening of a marine gateway between 2
Tasmania and Antarctica (e.g. Müller et al., 2000a; Royer and Rollet, 1997). 3
Our Early Oligocene Paleo-DEM indicates good fits between predicted and 4
observed location of the paleo-shorelines along the North West Shelf, western 5
margin, southeastern (Bass Strait) and eastern margins (Fig. 4c). Shallow ma- 6
rine to fluvial conditions (Duddy, 2003; Langford et al., 1995) in the Murray 7
Basin are correctly predicted, as well as exposure of the Gulf of Carpentaria 8
above sea level. In the Great Australian Bight, our predicted shoreline is sit- 9
uated significantly further landward than the one reported by Langford et al. 10
(1995), with observations indicating erosion and a shift of depocenters basin- 11
ward into the Great Australian Bight (Hou et al., 2008, 2006). 12

4.4 Late Oligocene – late Middle Miocene (30–10.4 Ma) 13

Fast northward motion of Australia continued in the Early/Mid Miocene. For 14
that time period, we predict that the entire northern half of the continent was 15
affected by increasing negative dynamic topography related to the SE Asian 16
subduction zone system (Fig. 4d). Modelled amplitudes in the northern parts 17
of Australia reach up to -450 m, while the southern downwelling progressively 18
affects areas south of the continental margin. The western margin is situated 19
parallel to the zero dynamic topography contour, while the southern Australia 20
is placed over an E-W elongated band of less pronounced mantle downwelling. 21

A global sea level rise from the Early Oligocene to the Early Eocene (Fig. 2) 22
resulted in a marine transgression in the Late Oligocene, leading to a widespread 23
deposition of shallow-marine limestones and flooding of the marginal basins 24

around Australia in the Miocene (Langford et al., 1995). Modelled paleo- 1
shorelines at 15 Ma (Early/Mid Miocene) match Langford et al.’s interpre- 2
tation well along the North West Shelf, the western margin, the southeastern 3
and eastern margins (Fig. 4d). We over-predict elevations in the Eucla Basin, 4
which was inundated during the Latest Oligocene until the Mid Miocene, 5
and the northern margin off the Northern Territory, resulting in modelled 6
subaerial exposure where shallow marine conditions are reported (Langford 7
et al., 1995). Flooding along the southern parts of the Carpentaria Basin are 8
also over-predicted, causing our modelled paleo-shoreline to be located too 9
far landward. In the Murray Basin our predicted elevation agrees with the 10
reported deposition of shallow marine/epicontinental limestones (McGowran 11
et al., 2004; Lukasik and James, 2003). 12

4.5 Late Miocene (10.4–5.3 Ma) 13

The continued northward motion of the Australian continent at relatively high 14
plate velocities towards the SE Asian slab burial ground resulted in further 15
increase of the area affected by negative dynamic topography along Australia’s 16
northern margin (Fig. 4e). At this time, we predict that nearly all of Australia 17
is affected by downward-deflection of the surface topography due to mantle 18
convection. The E-W striking arch of less negative topography straddles the 19
southernmost Australian margin and dynamic topography amplitudes reach 20
-550 m in northern Australia and around -200 to -250m along the southern 21
margins (Fig. 4e). 22

Further lowering of global eustatic sea level in the Late Miocene resulted in 23
a repeated regression along most of the continental shelf and marginal basins 24

similar to that in the Early Oligocene (Langford et al., 1995). Our predicted 1
topography for the Late Miocene (8 Ma) largely agrees with paleogeographic 2
data along the northwestern, western and southeastern margin of Australia 3
(Fig. 4e). The topography of the Murray Basin is modelled as semicircular 4
depression elevated 10–50 m above sea level, in accordance with a Mid-Late 5
Miocene unconformity (Gallagher and Gourley, 2007). We predict too deep 6
bathymetry for the southern Gulf of Carpentaria, the northernmost margin, 7
the Bight margin and the northeastern margin, resulting in the modelled paleo- 8
shorelines being located too far landward. Along the northern margin, the 9
onset of the collision of the northern Australian margin with the Sunda Trench 10
(Hall, 2002) and the associated flexural response (Harrowfield and Keep, 2005) 11
might have overprinted any signature from dynamic topography and eustatic 12
sea level changes. 13

4.6 Pliocene (5.3–1.6 Ma) 14

Collision along the northern Australian plate margin with the subduction zone 15
arc system of SE Asia had already commenced during the Miocene (Hall, 16
2002). Our modelled dynamic topography for the Pliocene time slice is char- 17
acterised by further increase in negative amplitudes for the northern to cen- 18
tral parts of the continent as northward motions at relatively high velocities 19
continue (Fig. 4f). Predicted amplitudes increased to around -600 m along 20
the northern margin. However, the dynamic topography with amplitudes of 21
around -250 m along the southern margin did not change markedly over the 22
past 15 Ma. 23

The gradual change from the Late Miocene to Pliocene paleogeography is well 24

reflected in our predicted topography of the Australian continent at 3 Ma 1
(Fig. 4f). There is broad agreement between our modelled and the interpreted 2
paleo-shorelines (Langford et al., 1995) along all continental margins and most 3
marginal basins. We over-estimate the topography of the Murray Basin by 10– 4
50m as indicated by a rapid marine transgression and subsequent deposition 5
of shallow marine muds and barrier sand complexes in the southwestern and 6
central parts of the basin (Langford et al., 1995; Roy et al., 2000). Fishwick 7
et al. (2005); Finn et al. (2005); Simons et al. (1999) suggest a thin litho- 8
sphere which is altered and infiltrated by volatiles due to subduction along 9
the Australian Pacific margin and opening of the Tasman Sea in the late Cre- 10
taceous (Gaina et al., 1998). These heterogeneities occur above our 220 km 11
depth model-cut off and hence might not have been appropriately accounted 12
for (cf. Section 3.1). 13

5 Vertical motions of the Australian continent 14

By combining dynamic topography models with eustatic sea level variations 15
and local tectonic subsidence analysis based of published well data, the vertical 16
motions of the Australian continent can be estimated. We have modelled the 17
elevation history of four different wells situated in low elevations on the passive 18
margins or close vicinity, located in the Gulf of Carpentaria, the North West 19
Shelf, the Eucla and Murray Basins. 20

The tectonic subsidence of the Carpentaria Basin, represented by the Duyken- 21
1 well (Fig. 6a), exhibits gradual tectonic subsidence throughout the Tertiary, 22
punctuated by a rapid subsidence pulse between about 38 and 30Ma. The grad- 23
ual background tectonic subsidence throughout the Tertiary is unexpected for 24

this epicratonic basin - no significant thermal subsidence during the Tertiary 1
is expected. According our mantle convection model, this area has experienced 2
continued slow subsidence during the Tertiary (Fig. 6a), roughly matching the 3
observed tectonic subsidence in this area if we exclude the sharp subsidence 4
pulse between 38 and 30 Ma, thus providing a favourable match between ob- 5
servations and model. The cause for the rapid subsidence pulse is enigmatic 6
as the onset of collision processes in Papua New Guinea only starts in Mid- 7
Oligocene times. 8

The Carnarvon Basin is well known to show anomalous, gradual accelerated 9
tectonic subsidence in the Late Tertiary (Müller *et al.*, 2000b), even though it 10
is located over 1000 km away from the Sunda Trench, ruling out flexural plate 11
bending influence on tectonic subsidence. The last rifting episode affecting 12
the region was the India-Australia breakup in early Cretaceous times (Exon 13
and Colwell, 1994). Well Urala-1 in the Carnarvon Basin shows accelerated 14
tectonic subsidence after 36 Ma (Fig. 5b). The subsidence anomaly for the 15
entire time period after 38 Ma is of the order of 150 m (Fig. 5b). Our dynamic 16
topography model (Fig. 5b) predicts about the same amount of subsidence 17
for this location, originating from the growing influence of the slab material 18
sinking underneath northern Australia during this time period (Fig. 4c), as 19
Australia continues to move towards the Melanesian subduction system at 20
speeds over 60 mm/yr (Fig. 4c-4a). 21

In the eastern onshore Eucla Basin, the Mallabie-1 well also shows continuous 22
tectonic subsidence over the past 70 Ma with a minor phase of accelerated 23
subsidence between 36 and 30 Ma. The well is located in the vicinity to the 24
southern Australian passive margin and hence was subtly affected by the rift- 25
ing between Australia and Antarctica (c.f. Brown *et al.*, 2001). We interpret 26

the subsidence until 36 Ma to be dominated by decaying thermal subsidence 1
related to the Australia-Antarctica breakup. However, the observed continued 2
tectonic subsidence (Fig. 6c) in post-Eocene times points towards anomalous 3
subsidence. Our modelled dynamic topography for the period between 36 Ma 4
and present-day indicates the generation of about 150 m of additional accom- 5
modation space due to mantle effects. 6

The Murray basin (North Renmark-1 well, Fig. 6d) exhibits gradual tectonic 7
subsidence totalling about 100m, from 66 to 37 Ma, even though this area 8
is not known to have experienced any crustal thinning during the rift-phase 9
between Australia and Antarctica – the Murray basin is merely an intracon- 10
tinental area inundated by shallow seas at various times during the Tertiary 11
([Lukasik et al., 2000](#)). This raises the question why it should display tectonic 12
subsidence during the Early Tertiary. A strong, accelerated subsidence pulse 13
of nearly 200 ± 50 m is seen between 38 and 30 Ma. The short wavelength of 14
this pulse precludes it being caused entirely by mantle-driven dynamic topog- 15
raphy, however, another pulse of accelerated topography occurs in the last 10 16
million years. The water depth errors (Fig. 6d) would allow these two pulses 17
to be less extreme, with continued accelerated subsidence occurring in the 18
period between 30 and 10 Ma. Our dynamic topography model (Fig. 6d) pre- 19
dicts roughly the observed magnitude of tectonic subsidence both between 66 20
and 38 Ma, as well as after 10 Ma, providing convincing evidence that most 21
observed Tertiary tectonic subsidence of the area, with the exception of the 22
rapid subsidence pulse from 38 to 30 Ma, is indeed mantle convection driven. 23

6 Summary and discussion

1

The Australian Cenozoic surface topography has been significantly altered by transient, mantle convection–induced surface displacement and eustatic sea level changes. Using an integrated method which combines dynamic topography models with eustatic sea level estimates, plate kinematics, and geological observations, we can model spatial and temporal changes in the paleogeography of Australia which are well in agreement with the observed geological record. Matching of paleogeographic data with a dynamic topography model based on the S20RTS seismic tomographic model (Ritsema et al., 1999) and the sea level estimate by Haq and Al-Qahtani (2005), the maximum amplitudes of dynamic topography affecting the Australian region during the Cenozoic can be estimated to be in the order of 500–600 m.

2

3

4

5

6

7

8

9

10

11

12

The Australian continent has been situated in the interior of the Indo-Australian plate during most of the Cenozoic. Hence plate boundary processes did not directly affect the topography of the continent, making it an ideal place to study the influence of deep Earth processes on surface dynamics. Only the recent collision with the Southeast Asian subduction system affected large parts of the northern Australian margin due to flexural loading. Localised and regional tectonic processes such as a changing Cenozoic intraplate stress regime (Dyksterhuis and Müller, 2008; Dyksterhuis et al., 2005; Célerier et al., 2005; Sandiford et al., 2004; Coblentz et al., 1995), rifting and wrench tectonics (along the southern Australian margin in the Cretaceous/Earliest Tertiary; Norvick and Smith (2001)), flexure (Haddad and Watts (1999) in northern Australia; Quigley et al. (2007); Célerier et al. (2005) in South Australia) and volcanism (Pliocene–Pleistocene, southeast Australia; Demidjuk et al. (2007);

13

14

15

16

17

18

19

20

21

22

23

24

25

Roy et al. (2000)) are other likely causes for surface deflection. However, these processes usually affect smaller areas and yield different geometrical patterns (e.g. narrow, elongated depressions due to foreland loading) compared to the continent-scale inundation patterns we focus on in this study. Low-amplitude localised surface deflections do not have a significant impact on the continental inundation patterns.

The falling global eustatic sea level in the Cenozoic is counterbalanced and partly outpaced by the effect of an increasing negative dynamic topography in the Australian region, due to the motion of Australia toward the long-term Tethyan/Pacific slab burial ground in Southeast Asia. Fig. 6 shows the modelled elevation for four wells, comparing our predicted elevation with the paleo-environment indicators (submerged, depositional vs. elevated, erosional) as reported by Langford et al. (1995). Our models successfully predict the Cenozoic paleo-elevation history for all four locations, both qualitatively and quantitatively. Data from the North Renmark 1 (Fig. 6d) and Mallabie 1 (Fig. 6c) locations in the Murray and Eucla Basin, respectively, indicates clearly shallow marine to low subaerial exposure for both locations, most likely not exceeding 60 m of water depths (e.g. Lukasik et al., 2000) in the Murray Basin, and marginal marine to fluvial environments with partly glauconitic facies for the eastern Eucla Basin (Hou et al., 2006). Lacking detailed stratigraphic data for the Duyken-1 (Fig. 6a) and Urala-1 (Fig. 6b) wells do not allow a rigorous quantitative assessment of our modelled paleo-elevations, however, reported unconformities and depositional cycles indicate a good fit.

The differences between our modelled topography and the observed paleogeography based on Langford et al. (1995) are expressed by calculating the area between modelled and observed paleo-shorelines through time and deriving

the amount of inundation relative to the present-day 200 m isobath (Fig. 7).
A particularly good fit for the whole continent is achieved for ages > 60 Ma,
36–31 Ma, and 11–9 Ma. Between 60–36 Ma, our models differ by up to 7%
from the computed inundation based on [Langford et al. \(1995\)](#). Similarly, the
period between 30–11 Ma shows up to 20% difference between predicted and
observed inundation. Responsible for these big discrepancies between model
and observations is the fact, that the flooding of the vast Eucla basin, both
during Eocene and Miocene is not reproducible with our models. We attribute
this mismatch to processes in the lithosphere, which are not taken into account
in our models. [DiCaprio et al. \(2009\)](#) also observed that short wavelength sig-
nals, not predicted by mantle convection models, are required in order to
predict the flooding history of the Eucla Basin.

7 Conclusions

The approach of integrating mantle convection-induced dynamic topography,
eustatic sea level variations, plate kinematic and geologic data provides a
powerful method to investigate the dynamic Earth system. It allows to quali-
tatively and quantitatively assess the dynamic paleogeography of stable con-
tinental platforms, the contribution of mantle-induced surface topography on
observed regional anomalous epeirogenic processes and with it the changes
occurring in the erosional domains, the sediment routing and depositional
systems.

In particular, our model suggests that:

- From the Paleocene to the Eocene Australia gradually moved over a dy-

namic topography low which was centered around the Canning Basin area 1
 at the beginning of the Tertiary, driven by a slow northwestward absolute 2
 motion of Australia from about 65 to 45 Ma. This process resulted in a 3
 gradual uplift of the Northwest Shelf paired with subsidence of the Great 4
 Australian Bight area. The mantle downwelling is interpreted to reflect sink- 5
 ing slab material originally subducted along Australia’s Cretaceous eastern 6
 Gondwana margin. 7

- Accelerated northward motion of Australia after 45 Ma shifted this dynamic 8
 topography low offshore to the Southern Ocean, contributing to a regression 9
 in the central Eucla Basin from the Late Eocene to the Mid-Oligocene, but 10
 the magnitude of the observed Eocene transgression and regression is not 11
 well captured in our model. 12
- From the Mid-Oligocene to the Mid-Miocene Australia’s continued fast 13
 northward motion progressively placed the Gulf of Carpentaria and the 14
 Cape York Peninsula over the Melanesian slab burial ground, drawing down 15
 the entire northern half of the Australian continent, while southern Aus- 16
 tralia was placed over an east-west elongated band of less pronounced man- 17
 tle downwelling. This resulted in moderate regional uplift, paired with a 18
 global sea level rise in the Early Miocene of similar magnitude. 19
- In post–Mid-Miocene times, the northern dynamic topography low progres- 20
 sively affected areas further south, reaching latitudes of about 30° S as 21
 Australia progressively moved northwards over subducted slab material. 22
 However, the dynamic topography amplitudes along the southern coast did 23
 not change markedly over the last 15 Myrs according to our model, im- 24
 plying a north-down scenario rather than a tilting of the entire Australian 25
 continent during this period. 26
- Combined with a falling global sea level, the relative lack of change in dy- 27

1 namic topography since the Mid-Miocene resulted in renewed exposure of
2 the Eucla Basin, paired with a transgression in the Gulf of Carpentaria,
3 where subsidence rates exceeded rates of long-term sea level fall.

4 Our model predicts an overall flooding history for the Australian continent
5 which agrees with most of the geological observations. We demonstrate that
6 the northward motion of the Australian continent resulted in large lateral dis-
7 placement relative to the underlying mantle which induced complex warping
8 of the Australian surface topography over the past 70 Ma where. Changes in
9 eustatic sea level were largely counterbalanced and partly outweighed by dy-
10 namic topography, affecting the flooding history of large epicontinental basins
11 such as the Gulf of Carpentaria, the Murray-Darling basin and the Eucla
12 basin. Based on our modelling, we conclude that the mantle-induced surface
13 topography for the Australian continent during the Cenozoic was not larger
14 than 600 m in amplitude and in average similar to the amplitudes of eustatic
15 sea level change.

16 We are not able to reproduce the overall transgression and regression patterns
17 in the Eucla Basin along the Great Australian Bight. This indicates that
18 shallow lithospheric heterogeneities might have played a more dominant role,
19 which might have been related to the style of passive margin evolution and
20 early spreading history in the Australia-Antarctica system.

21 Our results have implications not only for reconstructing the creation and de-
22 struction of sediment accommodation space, but also for understanding the
23 effects of deep Earth dynamics on the evolution of sediment source- and rout-
24 ing systems and the depositional architecture in large intracontinental basins.

Acknowledgements We acknowledge Mike Sandiford for valuable discussions on the Australian flooding history. Nicholas Rawlinson and Wouter Schellart are thanked for editorial assistance. An anonymous reviewer and Mark Quigley provided many constructive remarks and helped to significantly improve the manuscript. This work was partly funded by an ARC linkage grant with ExxonMobil Upstream Research. Figures for this publication have been generated using the Generic Mapping Tools ([Wessel and Smith, 1998](#)). The electronic supplementary information contains two [QuickTime](#) animations.

References

- Allen, P. A., Allen, J. R., 2005. Basin Analysis: Principles and Applications, 2nd Edition. Blackwell Publishing, Incorporated, Oxford OX4 1JF, United Kingdom.
- Artemieva, I. M., 2003. Lithospheric structure, composition, and thermal regime of the East European Craton: implications for the subsidence of the Russian Platform. *Earth Planet. Sci. Lett.* 213, 431–446.
- Berggren, W. A., Kent, D. V., Swisher III, C. C., Aubry, M. P., 1995. A revised Cenozoic geochronology and chronostratigraphy. In: Berggren, W. A., et al. (Eds.), *Geochronology, Time Scales, and Global Stratigraphic Correlation*. Vol. 54 of Special Publication. SEPM Soc. Sediment. Geol., pp. 129–212.
- Bond, G. C., 1978. Speculations on real sea-level changes and vertical motions of continents at selected times in the Cretaceous and Tertiary periods. *Geology* 6, 247–250.
- Brown, B., Müller, R. D., Struckmeyer, H. I. M., 2001. Anomalous Tectonic Subsidence of the Southern Australian Passive Margin: Response to Cretaceous Dynamic Topography or Differential Lithospheric Stretching? In:

- PESA Eastern Australian Basins Symposium, Melbourne, Vic, 25-28 Nov. 1
2001. pp. 563–570. 2
- Burgess, P. M., Gurnis, M., 1995. Mechanisms for the formation of cratonic 3
stratigraphic sequences. *Earth Planet. Sci. Lett.* 136, 647–663. 4
- Célerier, J., Sandiford, M., Hansen, D. L., Quigley, M., 2005. Modes of active 5
intraplate deformation, Flinders Ranges, Australia. *Tectonics* 24, TC6006. 6
- Christie-Blick, N., Driscoll, N. W., 1995. Sequence Stratigraphy. *Ann. Rev.* 7
Earth Planet. Sci. 23 (1), 451–478. 8
- Clarke, J. D. A., Gammon, P. R., Hou, B., Gallagher, S. J., 2003. Middle to Up- 9
per Eocene stratigraphic nomenclature and deposition in the Eucla Basin. 10
Aust. J. Earth Sci. 50 (2), 231–248, doi 10.1046/j.1440–0952.2003.00995.x. 11
- Cluzel, D., Aitchison, J. C., Picard, C., 2001. Tectonic accretion and under- 12
plating of mafic terranes in the Late Eocene intraoceanic fore-arc of New 13
Caledonia (Southwest Pacific): geodynamic implications. *Tectonophysics* 14
340 (1-2), 23–59. 15
- Coblentz, D. D., Sandiford, M., Richardson, R. M., Zhou, S., Hillis, R. R., 16
1995. The origins of the intraplate stress field in continental Australia . 17
Earth Planet. Sci. Lett. 133, 299–309. 18
- Conrad, C. P., Gurnis, M., 2003. Seismic tomography, surface uplift, and 19
the breakup of Gondwanaland: Integrating mantle convection backwards 20
in time. *Geochem. Geophys. Geosyst.* 4 (3), 1031. 21
- Conrad, C. P., Lithgow-Bertelloni, C., Louden, K. E., 2004. Iceland, the Far- 22
allon slab, and dynamic topography of the North Atlantic. *Geology* 32 (3), 23
177–180. 24
- de Broekert, P., Sandiford, M., 2005. Buried Inset-Valleys in the Eastern Yil- 25
garn Craton, Western Australia: Geomorphology, Age, and Allogenic Con- 26
trol. *J. Geol.* 113 (4), 471–493. 27

- Demidjuk, Z., Turner, S., Sandiford, M., George, R., Foden, J., Etheridge, 1
M., 2007. U-series isotope and geodynamic constraints on mantle melting 2
processes beneath the Newer Volcanic Province in South Australia. *Earth* 3
Planet. Sci. Lett. 261 (3-4), 517–533. 4
- DiCaprio, L., Gurnis, M., Müller, R. D., 2009. Long-wavelength tilting of the 5
Australian continent since the Late Cretaceous. *Earth Planet. Sci. Lett.* 278, 6
175–185. 7
- Duddy, I. R., 2003. Mesozoic: a time of change in tectonic regime. In: Birch, 8
W. D. (Ed.), *Geology of Victoria. Special Publication 23. Geological Society* 9
of Australia (Victoria Division), Ch. 9, pp. 239–286. 10
- Dyksterhuis, S., Müller, R. D., 2008. Cause and evolution of intraplate orogeny 11
in Australia. *Geology* 36 (6), 495–498. 12
- Dyksterhuis, S., Müller, R. D., Albert, R. A., 2005. Paleostress field evolution 13
of the Australian continent since the Eocene. *J. Geophys. Res.* 110 (B5), 14
B05102. 15
- Exon, N. F., Colwell, J. B., 1994. Geological history of the outer North West 16
Shelf of Australia: a synthesis. *AGSO Journal of Australian Geology &* 17
Geophysics 15 (1), 177–190. 18
- Finn, C. A., Müller, R. D., Panter, K. S., 2005. A Cenozoic diffuse alkaline 19
magmatic province (DAMP) in the southwest Pacific without rift or plume 20
origin. *Geochem. Geophys. Geosyst.* 6 (2), Q02005. 21
- Fishwick, S., Heintz, M., Kennett, B. L., Reading, A. M., Yoshizawa, K., 22
2008. Steps in lithospheric thickness within eastern Australia, evidence from 23
surface wave tomography. *Tectonics* 27, TC4009. 24
- Fishwick, S., Kennett, B. L., Reading, A. M., 2005. Contrasts in lithospheric 25
structure within the Australian craton—insights from surface wave tomog- 26
raphy. *Earth Planet. Sci. Lett.* 231, 163–176. 27

- Gaina, C., Müller, R. D., 2007. Cenozoic tectonic and depth/age evolution of the Indonesian gateway and associated back-arc basins. *Earth-Science Rev.* 83, 177–203.
- Gaina, C., Müller, R. D., Royer, J.-Y., Stock, J., Hardebeck, J., Symonds, P., June 1998. The tectonic history of the Tasman Sea: A puzzle with 13 pieces. *J. Geophys. Res.* 103 (B6), 12413–12433.
- Gallagher, S. J., Gourley, T. L., 2007. Revised Oligo-Miocene stratigraphy of the Murray Basin, southeast Australia. *Aust. J. Earth Sci.* 54, 837–849.
- Gradstein, F., Ogg, J., Smith, A., Agterberg, F., Bleeker, W., Cooper, R., Davydov, V., Gibbard, P., Hinnov, L., House, M., Lourens, L., Luterbacher, H., McArthur, J., Melchin, M., Robb, L., Shergold, J., Villeneuve, M., Wardlaw, B., Ali, J., Brinkhuis, H., Hilgen, F., Hooker, J., Howarth, R., Knoll, A., Laskar, J., Monechi, S., Plumb, K., Powell, J., Raffi, I., Röhl, U., Sadler, P., Sanfilippo, A., Schmitz, B., Shackleton, N., Shields, G., Strauss, H., Van Dam, J., van Kolfschoten, T., Veizer, J., Wilson, D., 2004. *A Geologic Time Scale*. Cambridge University Press.
- URL <http://www.stratigraphy.org>
- Grand, S. P., van der Hilst, R. D., Widiyantoro, S., April 1997. Global seismic tomography; a snapshot of convection in the Earth. *GSA Today* 7 (4), 1–7.
- Gurnis, M., 1990. Bounds on global dynamic topography from Phanerozoic flooding of continental platforms. *Nature* 344, 754–756.
- Gurnis, M., 2001. Sculpting the Earth from Inside Out. *Sci. Amer.* 284, 40–48.
- Gurnis, M., Müller, R. D., Moresi, L. N., March 1998. Cretaceous Vertical Motion of Australia and the Australian–Antarctic Discordance. *Science* 279, 1499–1504.
- Haddad, D., Watts, A. B., 1999. Subsidence history, gravity anomalies, and flexure of the northeast Australian margin in Papua New Guinea. *Tectonics*

- 18 (5), 827–842. 1
- Hager, B. H., O’Connell, R. J., 1981. A simple global model of plate dynamics 2
and mantle convection. *J. Geophys. Res.* 86, 4843–4867. 3
- Hall, R., 1998. The plate tectonics of Cenozoic SE Asia and the distribution 4
of land and sea. In: Hall, R., Holloway, J. D. (Eds.), *Biogeography and* 5
Geological evolution of SE Asia. Blackhuys Publisher, Leiden, pp. 99–131. 6
- Hall, R., April 2002. Cenozoic geological and plate tectonic evolution of SE 7
Asia and the SW Pacific: computer-based reconstructions, model and ani- 8
mations. *J. Asian Earth Sci.* 20 (4), 354–431. 9
- Hall, R., Wilson, M. E. J., 2000. Neogene sutures in eastern Indonesia. *J.* 10
Asian Earth Sci. 18, 781–808. 11
- Hallam, A., 1984. Pre-Quaternary Sea-Level Changes. *Ann. Rev. Earth* 12
Planet. Sci. 12, 205–243. 13
- Haq, B. U., Al-Qahtani, A. M., 2005. Phanerozoic cycles of sea-level change 14
on the Arabian Platform. *GeoArabia* 10 (2), 127–160. 15
- Haq, B. U., Hardenbol, J., Vail, P. R., 1987. Chronology of fluctuating sea 16
levels since the Triassic. *Science* 235, 1156–1167. 17
- Harrowfield, M. J., Keep, M., 2005. Tectonic modification of the Australian 18
North-West Shelf: episodic rejuvenation of long-lived basin divisions. *Basin* 19
Research 17, 225–239. 20
- Hinschberger, F., Malod, J.-A., Réhault, J.-P., Villeneuve, M., Royer, J.-Y., 21
Burhanuddin, S., 2005. Late Cenozoic geodynamic evolution of eastern In- 22
donesia. *Tectonophysics* 404, 91–118. 23
- Hou, B., Alley, N. F., Frakes, L. A., Stoian, L., Cowley, W. M., 2006. 24
Eocene stratigraphic succession in the Eucla Basin of South Australia and 25
correlation to major regional sea-level events. *Sed. Geol.* 183, 297–319, 26
doi:10.1016/j.sedgeo.2005.10.007. 27

- Hou, B., Frakes, L. A., Sandiford, M., Worrall, L., Keeling, J., Alley, N. F., 1
2008. Cenozoic Eucla Basin and associated palaeovalleys, southern Australia 2
– Climatic and tectonic influences on landscape evolution, sedimentation 3
and heavy mineral accumulation. *Sedimentary Geology* 203 (1-2), 112–130. 4
- Jordan, T. H., 1978. Composition and development of the continental tecto- 5
sphere. *Nature* 274, 544–548. 6
- Jordan, T. H., 1988. Structure and formation of the continental tectosphere. 7
J. Petrology Special Lithosphere Issue, 11–37. 8
- Kamp, P. J. J., 1986. The mid-Cenozoic Challenger Rift System of western 9
New Zealand and its implications for the age of Alpine fault inception. *Geol.* 10
Soc. Am. Bull. 97 (3), 255–281. 11
- Karato, S., 1993. Importance of anelasticity in the interpretation of seismic 12
tomography. *Geophys. Res. Lett.* 20, 1623–1626. 13
- Langford, R., Wilford, G., Truswell, E. M., Isern, A. R. (Eds.), 1995. Paleo- 14
geographic Atlas of Australia. Volume 10 – Cainozoic. Australian Geological 15
Survey Organization, Canberra. 16
- Lithgow-Bertelloni, C., Gurnis, M., 1997. Cenozoic subsidence and uplift of 17
continents from time-varying dynamic topography. *Geology* 25 (8), 735–738. 18
- Lithgow-Bertelloni, C., Silver, P. G., September 1998. Dynamic topography, 19
plate driving forces and the African superswell. *Nature* 395. 20
- Lukasik, J. J., James, N. P., September 2003. Deepening-upward subtidal cy- 21
cles Murray Basin, South Australia. *J. Sedim. Res.* 73 (5), 653–671. 22
- Lukasik, J. J., James, N. P., McGowran, B., Bone, Y., 2000. An epeiric ramp: 23
low-energy, cool-water carbonate facies in a Tertiary inland sea, Murray 24
Basin, South Australia. *Sedimentology* 47 (4), 851–881. 25
- McGowran, B., Holdgate, G. R., Li, Q., Gallagher, S. J., 2004. Cenozoic strati- 26
graphic succession in southeastern Australia. *Aust. J. Earth Sci.* 51 (4), 27

- 459–496. 1
- Miall, A. D., September 1992. Exxon global cycle chart: An event for every 2
occasion? *Geology* 20, 787–790. 3
- Miller, K. G., Kominz, M. A., Browning, J. V., Wright, J. D., Mountain, 4
G. S., Katz, M. E., Sugarman, P. J., Cramer, B. S., Christie-Blick, N., 5
Pekar, S. F., November 2005. The Phanerozoic Record of Global Sea-Level 6
Change. *Science* 310, 1293–1298. 7
- Mitrovica, J. X., Beaumont, C., Jarvis, G. T., 1989. Tilting of continental 8
interiors by the dynamical effects of subduction. *Tectonics* 8 (5), 1079–1094. 9
- Müller, R. D., Gaina, C., Tikku, A., Mihut, D., Cande, S. C., Stock, J. M., 10
2000a. Mesozoic/Cenozoic tectonic events around Australia. In: *The History 11
and Dynamics of Global plate motions*. Vol. 121 of *Geophys. Monogr. Ser.* 12
AGU, pp. 161–188. 13
- Müller, R. D., Lim, V. S. L., Isern, A. R., 2000b. Late Tertiary tectonic sub- 14
sidence on the northeast Australian passive margin: response to dynamic 15
topography? *Mar. Geol.* 162, 337–352. 16
- Müller, R. D., Sdrolias, M., Gaina, C., Roest, W. R., 2008a. Age, spread- 17
ing rates, and spreading asymmetry of the world’s ocean crust. *Geochem. 18
Geophys. Geosyst.* 9 (4), Q04006. 19
- Müller, R. D., Sdrolias, M., Gaina, C., Steinberger, B., Heine, C., 2008b. Long- 20
Term Sea-Level Fluctuations Driven by Ocean Basin Dynamics. *Science* 21
319 (5868), 1357–1362. 22
- Nielsen, S. B., Stephenson, R., Thomsen, E., 2007. Dynamics of Mid- 23
Palaeocene North Atlantic rifting linked with European intra-plate defor- 24
mations. *Nature* 450 (7172), 1071–1074. 25
- Nielsen, S. B., Thomsen, E., Hansen, D. L., Clausen, O. R., 2005. Plate-wide 26
stress relaxation explains European Palaeocene basins inversions. *Nature* 27

435, 195–198. 1

N.O.A.A., National Geophysical Data Center, 2006. ETOPO2v2 2-minute 2
 global relief. 3

URL <http://www.ngdc.noaa.gov/mgg/fliers/06mgg01.html> 4

Norvick, M. S., Smith, M. A., 2001. Mapping the Plate Tectonic Reconstruc- 5
 tion of Southern and Southeastern Australia and Implications for Petroleum 6
 Systems. *APPEA Journal* 49 (1), 15–35. 7

O’Neill, C., Müller, R. D., Steinberger, B., 2003. Geodynamic implications 8
 of moving Indian Ocean hotspots. *Earth Planet. Sci. Lett.* 215, 151–168, 9
 doi:10.1016/S0012-821X(03)00368-6. 10

Quigley, M. C., Sandiford, M., Cupper, M. L., 2007. Distinguishing tectonic 11
 from climatic controls on range-front sedimentation. *Basin Research* 19, 12
 491–505. 13

Ritsema, J., van Heijst, H. J., Woodhouse, J. H., 1999. Complex shear wave 14
 velocity structure imaged beneath Africa and Iceland. *Science* 286, 1925– 15
 1928. 16

Roy, P. S., Whitehouse, J., Cowell, P. J., Oakes, G., 2000. Mineral Sands Oc- 17
 currences in the Murray Basin, Southeastern Australia. *Economic Geology* 18
 95, 1107–1128. 19

Royer, J.-Y., Rollet, N., 1997. Plate-tectonic setting of the Tasmanian region. 20
Aust. J. Earth Sci. 44 (5), 543–560. 21

Russell, M., Gurnis, M., 1994. The planform of epeirogeny: vertical motions 22
 of Australia during the Cretaceous. *Basin Research* 6, 63–76. 23

Sahagian, D., Jones, M., August 1993. Quantified Middle Jurassic to Pale- 24
 ocene eustatic variations based on Russian Platform stratigraphy: Stage 25
 level resolution. *Geol. Soc. Am. Bull.* 105, 1109–1118. 26

Sahagian, D., Pinous, O., Olferiev, A., Zakharov, V., September 1996. Eustatic 27

- Curve for the Middle Jurassic-Cretaceous Based on Russian Platform and
Siberian Stratigraphy: Zonal Resolution. AAPG Bulletin 80 (9), 1433–1458.
- Sahagian, D., Watts, A. B., 1991. Introduction to the special section on mea-
surement, causes and consequences of long-term sealevel change. J. Geophys.
Res. 96, 6585–6589.
- Sandiford, M., 2003a. Geomorphic constraints on the Late Neogene tectonics
of the Otway Range, Victoria. Aust. J. Earth Sci. 50 (1), 69–80.
- Sandiford, M., 2003b. Neotectonics of southeastern Australia: Linking the
Quaternary faulting record with seismicity and in situ stress. In: Hillis,
R. R., Müller, R. D. (Eds.), Evolution and Dynamics of the Australian
Plate. Vol. 22 of Geol. Soc. Aust. Spec. Publ. 22 and Spec. Paper Geol. Soc.
Am. 372. Geol. Soc. of Australia and Geol. Soc. of America, pp. 101–113.
- Sandiford, M., 2007. The tilting continent: a new constraint on the dynamic
topographic field from Australia. Earth Planet. Sci. Lett. 261, 152–161.
- Sandiford, M., Coblenz, D. D., Richardson, R. M., 1995. Ridge torques and
continental collision in the Indian-Australian plate. Geology 23 (7), 653 –
656.
- Sandiford, M., Wallace, M. W., Coblenz, D. D., 2004. Origin of the in situ
stress field in south-eastern Australia. Basin Research 16, 325–338.
- Sandwell, D. T., 2009. SRTM30_PLUS: SRTM30, Coastal & Ridge multibeam,
estimated topography.
URL ftp://topex.ucsd.edu/pub/srtm30_plus/
- Schellart, W., 2007. North-eastward subduction followed by slab detachment
to explain ophiolite obduction and Early Miocene volcanism in Northland,
New Zealand. Terra Nova 19 (3), 211–218.
- Schellart, W. P., Lister, G. S., Toy, V. G., 2006. A Late Cretaceous and Ceno-
zoic reconstruction of the Southwest Pacific region: Tectonics controlled by

- subduction and slab rollback processes. *Earth-Science Rev.* 76, 191–233. 1
- Sclater, J. G., Christie, P. A. F., July 1980. Continental Stretching: An Ex- 2
planation of the Post-Mid-Cretaceous Subsidence of the Central North Sea 3
Basin. *J. Geophys. Res.* 85 (B7), 3711–3739. 4
- Shapiro, S. S., Hager, B. H., Jordan, T. H., 1999. Stability and dynamics of 5
the continental tectosphere. *Lithos* 48, 115–133. 6
- Simons, F. J., van der Hilst, R. D., 2002. Age-dependent seismic thickness 7
and mechanical strength of the Australian lithosphere. *Geophys. Res. Lett.* 8
29 (11), doi:10.1029/2002GL014962. 9
- Simons, F. J., Zielhuis, A., van der Hilst, R. D., 1999. The deep structure of 10
the Australian continent from surface wave tomography. *Lithos* 48, 17–43. 11
- Spasojević, S., Liu, L., Gurnis, M., Müller, R. D., 2008. The case for dynamic 12
subsidence of the U.S. east coast since the Eocene. *Geophys. Res. Lett.* 35, 13
L08305. 14
- Steckler, M. S., Watts, A. B., 1978. Subsidence of the Atlantic-type continental 15
margin off New York. *Earth Planet. Sci. Lett.* 41 (1), 1–13. 16
- Steinberger, B., 2007. Effects of latent heat release at phase boundaries on flow 17
in the Earth’s mantle, phase boundary topography and dynamic topography 18
at the Earth’s surface. *Phys. Earth Planet. Int.* 164, 2–20. 19
- Steinberger, B., Calderwood, A. R., 2006. Models of large-scale viscous flow 20
in the Earth’s mantle with constraints from mineral physics and surface 21
observations. *Geophys. J. Int.* 167, 1461–1481. 22
- Steinberger, B., Schmeling, H., Marquart, G., 2001. Large-scale lithospheric 23
stress field and topography induced by global mantle circulation. *Earth* 24
Planet. Sci. Lett. 186, 75–91. 25
- Steinberger, B., Sutherland, R., O’Connell, R. J., 2004. Prediction of Emperor- 26
Hawaii seamount locations from a revised model of global plate motion and 27

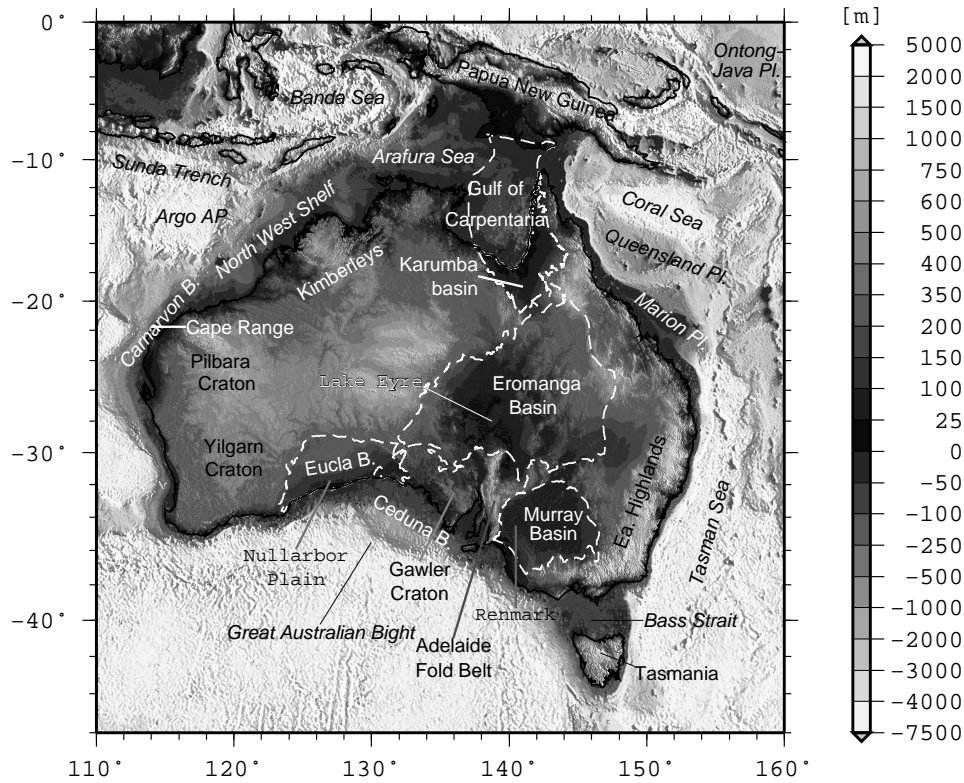
- mantle flow. *Nature* 430, 167–173. 1
- Stoddard, P. R., Abbot, D., 1996. Influence of the tectosphere upon plate 2
motions. *J. Geophys. Res.* 101 (B3), 5425–5433. 3
- Struckmeyer, H., Brown, P., 1990. Australian Sea Level Curves Part 1: Aus- 4
tralian Inundation Curves, Palaeogeography. Tech. rep., Bureau of Mineral 5
Resources, Geology and Geophysics Petroleum Division of the Australian 6
Mineral Industries Research Association, GPO Box 378, Canberra, ACT 7
2601 , Australia. 8
- Swain, C. J., Kirby, J. F., 2006. An effective elastic thickness map of Australia 9
from wavelet transforms of gravity and topography using Forsyth’s method. 10
Geophys. Res. Lett. 33, L02314. 11
- Trampert, J., Deschamps, F., Resovsky, J., Yuen, D. A., October 2004. Prob- 12
abilistic Tomography Maps Chemical Heterogeneities in the lower mantle. 13
Science 306, 853–856. 14
- van der Hilst, R. D., Widiyantoro, S., Engdahl, E. R., 1997. Evidence of deep 15
mantle circulation from global tomography. *Nature* 386, 578–584. 16
- Veevers, J. J. (Ed.), 1984. Phanerozoic Earth History of Australia. No. 2 in 17
Oxford Monographs on Geology and Geophysics. Clarendon Press, Oxford, 18
United Kingdom. 19
- Veevers, J. J., 2001. Billion-year earth history of Australia and neighbours in 20
Gondwanaland. GEMOC Press, Sydney, Australia. 21
- Watts, A. B., Thorne, J., November 1984. Tectonics, global changes in sea 22
level and their relationship to stratigraphical sequences at the US Atlantic 23
continental margin. *Mar. Petrol. Geol.* 1, 3–19. 24
- Wessel, P., Smith, W. H. F., 1998. New, improved version of Generic Mapping 25
Tools released. *EOS Trans. Am. Geophys. Union* 79 (47), 579. 26
- West, B. P., Wilcock, W. S. D., Sempéré, J.-C., Géli, L., 1997. Three- 27

dimensional structure of asthenospheric flow beneath the Southeast Indian 1
Ridge. *J. Geophys. Res.* 102 (B4), 7783—7802. 2

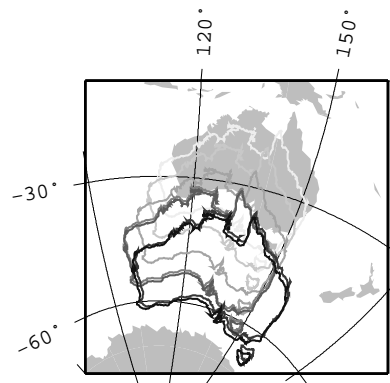
Wheeler, P., White, N., 2000. Quest for dynamic topography: Observations 3
from Southeast Asia. *Geology* 28 (11), 963–966. 4

Whittaker, J. M., Müller, R. D., Leitchenkov, G., Stagg, H. M. J., Sdrolias, 5
M., Gaina, C., Goncharov, A., 2007. Major Australian-Antarctic Plate Re- 6
organization at Hawaiian-Emperor Bend Time. *Science* 318, 83–86. 7

Xie, X., Müller, R. D., Lia, S., Gong, Z., Steinberger, B., 2006. Origin of 8
anomalous subsidence along the Northern South China Sea margin and its 9
relationship to dynamic topography. *Mar. Petrol. Geol.* 23, 745–765. 10



(a)



(b)

Figure 1. (a) Main morphological features of the greater Australian region based on the SRTM30_plus DEM (Sandwell, 2009). Coastlines indicated by thin black line, basin outlines as dashed white lines. Abbreviations: AP – Abyssal Plain; B. – Basin; Pl. – Plateau. Adelaide Fold Belt comprises the Flinders/Mt. Lofty Ranges; Carnarvon Basin area delineates the approximate location for the on- and offshore Carnarvon Basin/Carnarvon margin; Renmark denotes Renmark area in Murray basin; Ea. Highlands denotes Eastern Australian Highlands. (b) Plate tectonic history of the Australian Plate for the last 70 Ma. Coloring refers to the position of Australia in an absolute reference frame (Müller et al., 2008b) in 10 myr time steps from 70 Ma to present depicted as filled solid gray.

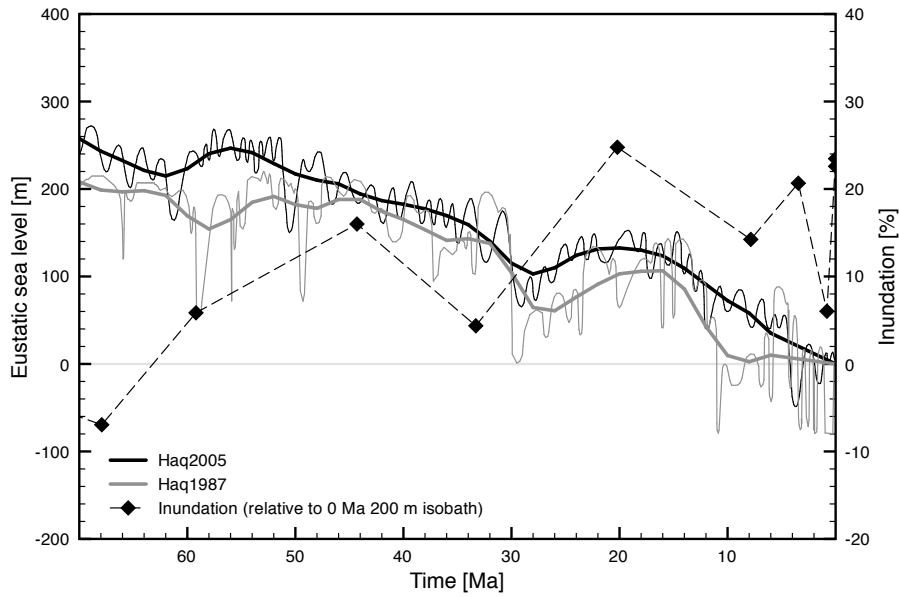
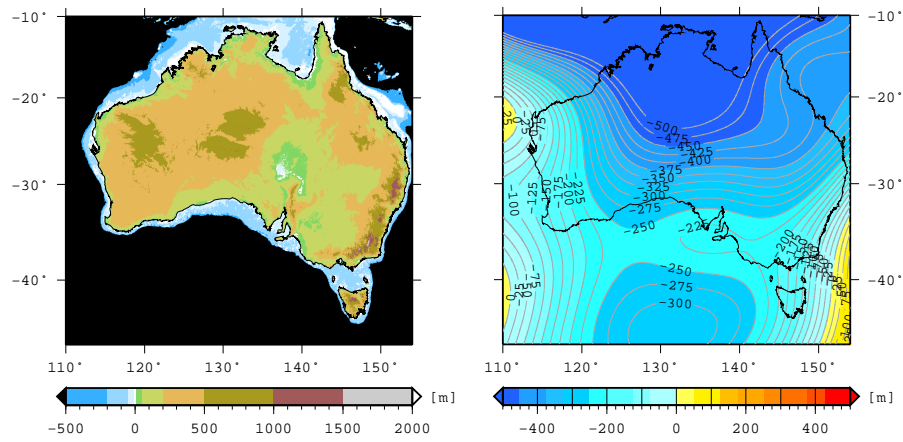
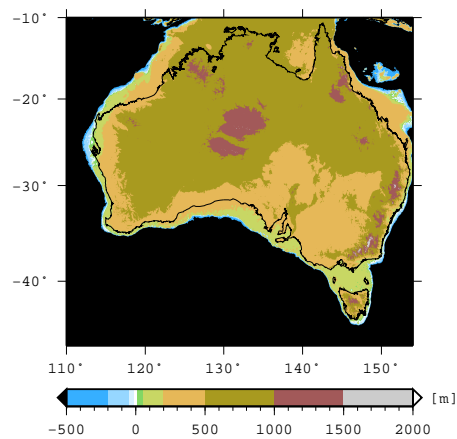


Figure 2. Global eustatic sea level curves and inundation history of the Australian continent based on paleoshorelines derived from [Langford et al. \(1995\)](#). Solid black curves based on [Haq and Al-Qahtani \(2005\)](#) sea level curve, with thin line representing the original estimate, thick line: filtered curve. Solid gray curves are based on [Haq et al. \(1987\)](#) sea level curve, with thin line representing original curve, thick line filtered curve. Filtered lines show long wavelength component of the eustatic sea level estimate using a cosine arch filter with 10 m.y. window. The amount of inundation is computed relative to the present-day 200 m isobath derived from the ETOPO2 global 2' topography ([N.O.A.A., National Geophysical Data Center, 2006](#)).



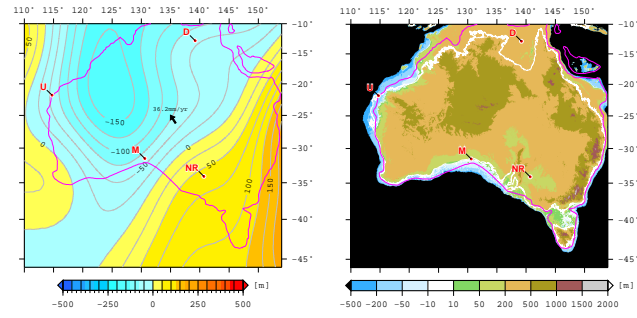
(a) DEM

(b) scaled dynamic topography

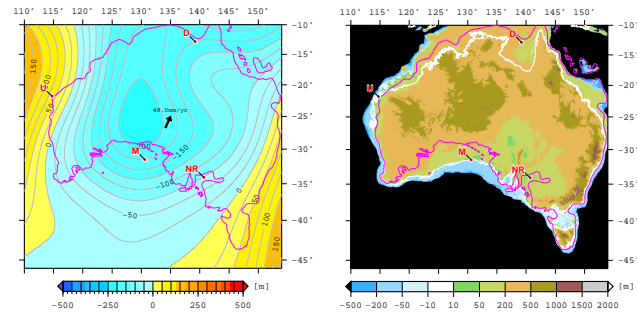


(c) DEM with dynamic topography
subtracted

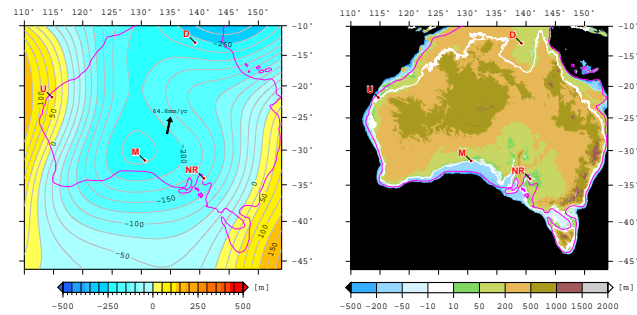
Figure 3. Present-day Australian topography, dynamic topography and difference topography. The topography with the dynamic component subtracted (Fig 3c) is used as base grid for topography reconstructions. (a) present-day surface topography; (b) Scaled dynamic topography; (c) DEM with dynamic topography component subtracted. Thin, black line is present-day coastline, figures (a) and (c) have the same colourscale.



(a) Mid Paleocene (61 Ma)

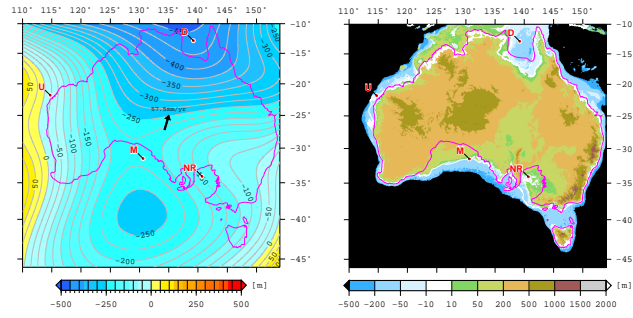


(b) Mid Eocene (43 Ma)

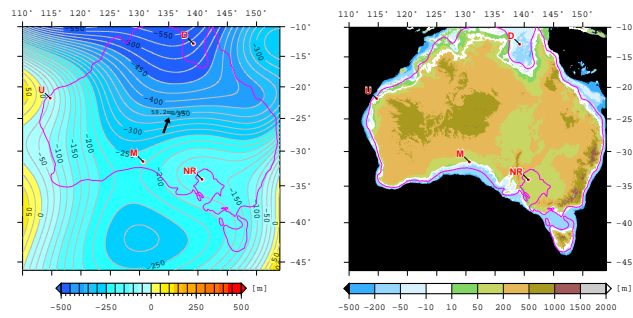


(c) Early Oligocene (32 Ma)

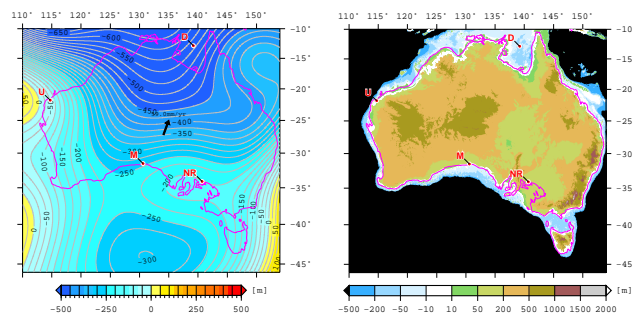
Figure 4. Dynamic topography and best-fit paleogeographic reconstructions, combining dynamic topography models, eustatic sea level variations and isostatic correction for sediments for six different times. Eustatic sea level is based on [Haq and Al-Qahtani \(2005\)](#) and isostatic correction uses sediment thickness based on well data from [Langford et al. \(1995\)](#). a) ≈ 61 Ma (Early Paleocene, Cenozoic 1 interval); b) ≈ 43 Ma (Mid Eocene, Cenozoic 2 interval); c) ≈ 32 Ma (Early Oligocene, Cenozoic 3 interval); Australia is kept fixed in present-day coordinates. Red line indicates paleo-shoreline position based on the combined interpreted “land” environments [Langford et al. \(1995\)](#) for each individual time slice. Black stars indicate wells for which a modelled elevation history is shown in Fig. 6.



(d) Mid Miocene (15 Ma)



(e) Late Miocene (8 Ma)



(f) Pliocene (3 Ma)

Figure 4. continued. d) \approx 15 Ma (Mid Miocene, Cenozoic 4 interval); e) \approx 8 Ma (Late Miocene, Cenozoic 5 interval); f) \approx 3 Ma (Pliocene, Cenozoic 6 interval).

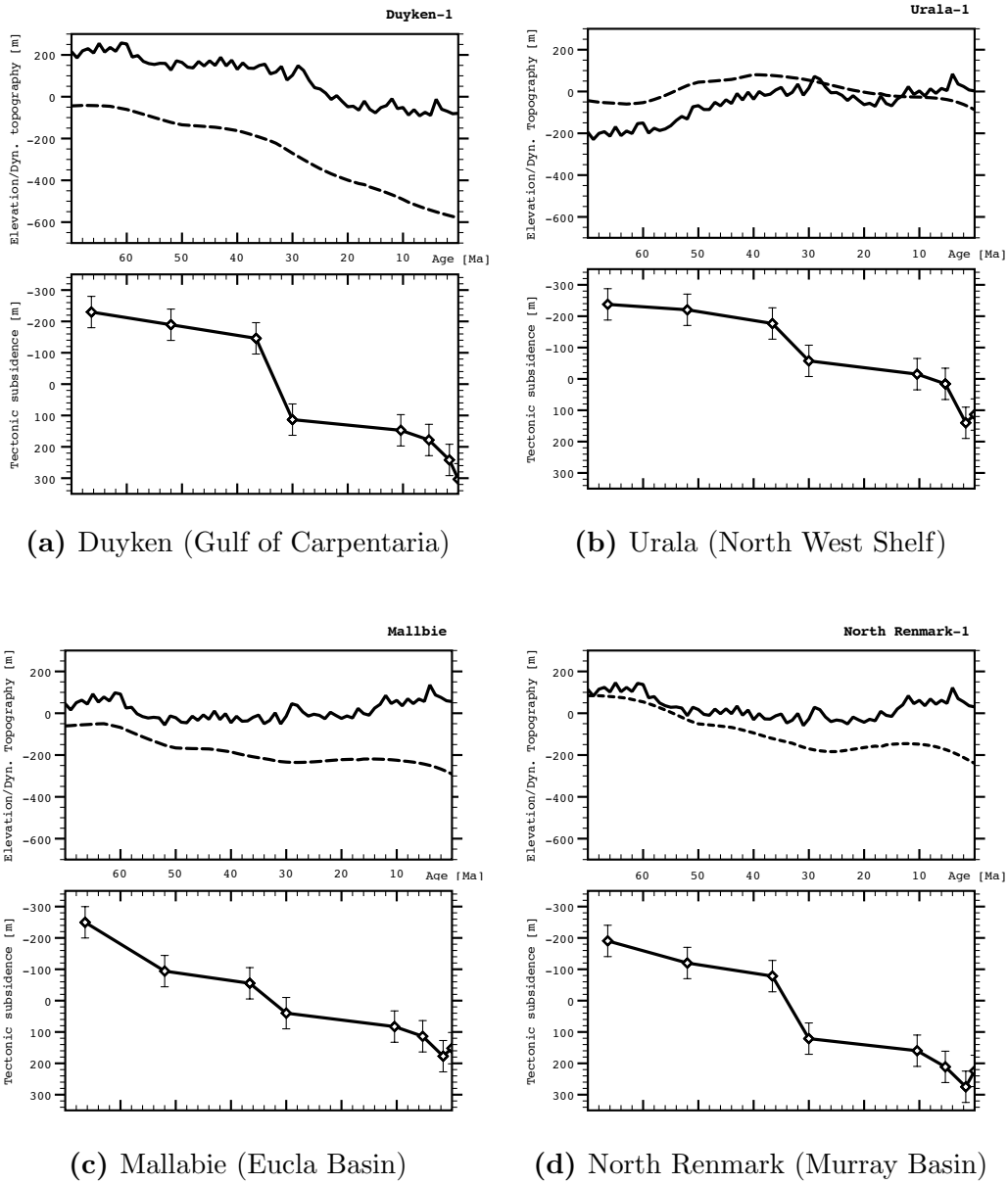


Figure 5. Scaled dynamic topography (upper plots, dashed line) reconstructed topography histories (upper plots, solid line), and tectonic subsidence adjusted for eustatic sea level (lower plot, solid line) for 4 selected wells for the last 70 Ma. (a) Duyken 1 well, Carpentaria Basin; (b) Urala 1 well, North Carnarvon Basin; (c) Mallbie well, eastern Eucla basin; (d) North Renmark-1 well, Murray Basin. Error bars in lower plots mark $\pm 50m$ uncertainty in paleo-water depth. For location of the wells see Fig. 6.

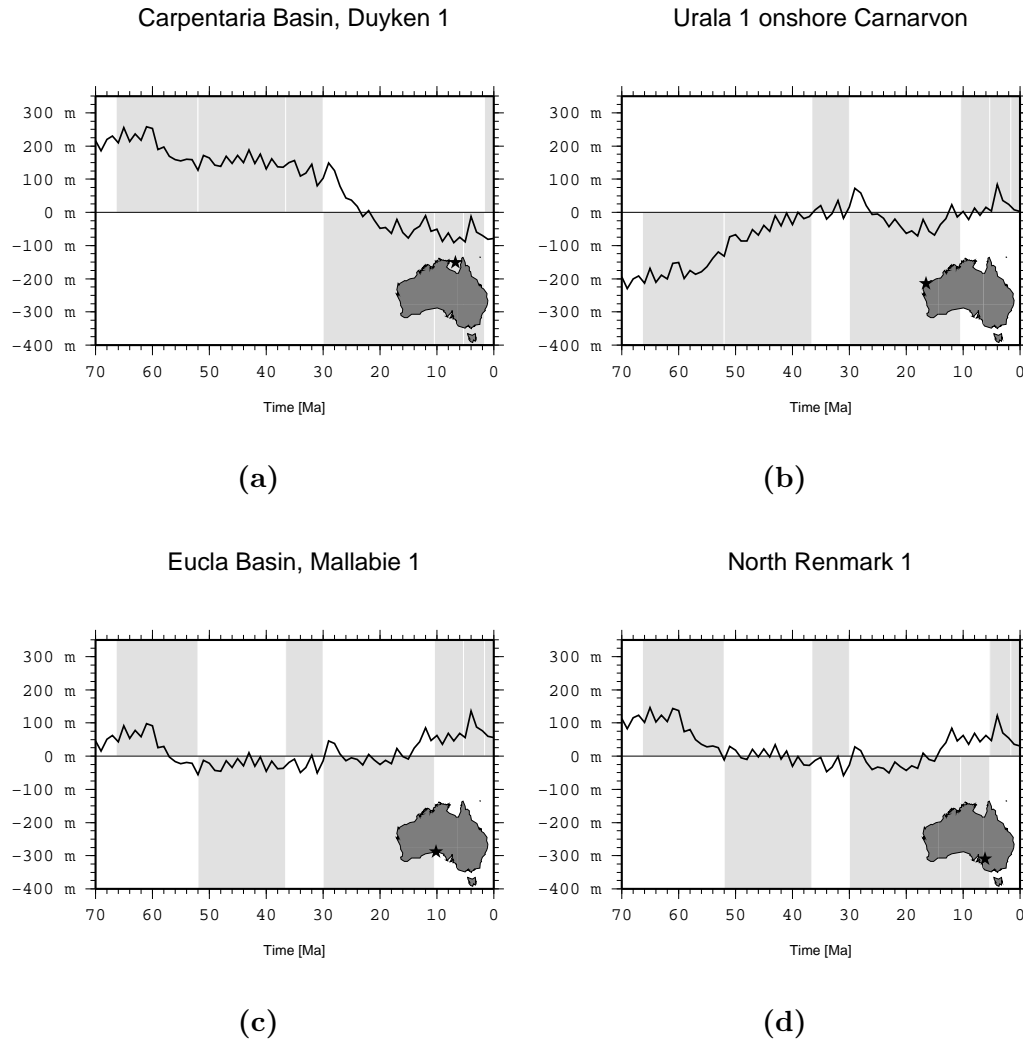


Figure 6. Elevation history relative to sea level of 4 wells in Australia using integrated model which combines dynamic topography, plate kinematics, eustatic sea level (Haq and Al-Qahtani, 2005) and sediment correction derived from Langford et al. (1995) and other sources. Gray rectangles in background indicate paleo-environment based on Langford et al. (1995) where a rectangle below 0 m elevation indicates flooding, and above 0 m indicates exposure above sea level for the respective location at given time. If the modelled curve is located within a gray rectangle, the observations are qualitatively matched. Dynamic topography model is scaled empirically by a factor of 0.55.

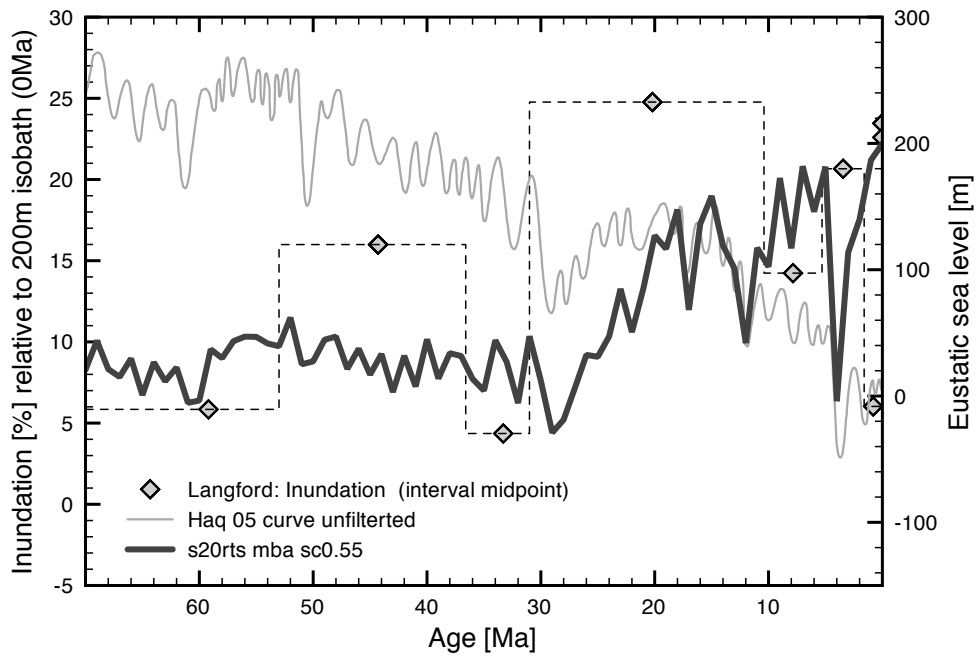


Figure 7. Inundation of the Australian continental area over the past 70 Ma using our integrated paleo-topography model. Dynamic topography input is scaled by a factor of 0.55. Inundation is measured as % of the total continental area above the present-day 200 m isobath which is flooded at any given time. Diamonds and thin black dashed line shows the inundation estimate using the observations from [Langford et al. \(1995\)](#). Solid gray line shows the eustatic sea level used ([Haq and Al-Qahtani, 2005](#)).